Waveguide Quantum Memory

W. Tittel (1), M. Afzelius (2), P. Baldi (3), N. Gisin (2), R. Ricken (4), S. Hastings-Simon (2), V. Scarani (2), H. Suche (4), W. Sohler (4), and M. Staudt (2)

1) Institute for Quantum Information Science, University of Calgary, Canada
2) Group of Applied Physics, University of Geneva, Switzerland
3) Laboratoire de Physique de la Matière Condensée, University of Nice-Sophia Antipolis, France
4) Angewandte Physik, University of Paderborn, Germany

Abstract: *We study Erbium doped LiNbO$_3$ waveguides for their suitability to store quantum information encoded into single photons, as required for a quantum repeater. Specifically, we perform stimulated photon-echo experiments for storage and readout of (classical) light pulses, which yield important information about the storage of single photon states. Furthermore, we investigate Stark-shift based line-shifts of the 1.53 μm transition, as required for a highly efficient quantum state storage protocol. Our findings demonstrate the potential of Er:LiNbO$_3$ waveguides for quantum state storage.*

Introduction

The last years have seen a remarkable advance of experimental quantum communication, in particular of quantum cryptography that promises information-theoretic secure communication [1]. Yet, many problems still have to be overcome before a quantum secured communication network will be available. A major challenge concerns the increase of the transmission distance, which is, among others, limited through the combination of absorption in the transmission channel and detector noise. In contrast to classical telecommunications, a direct amplification of a single-photon quantum state is impossible. The concept of a quantum repeater [2] is based on several key elements, which are the creation and distribution of entangled pairs of photons over sub-sections of the complete link, swapping to extend the entanglement over the whole channel, and quantum memories that allow increasing the efficiency of the overall process. The entanglement can then be used for any kind of quantum communication task, for instance for quantum cryptography.

Many schemes for storage of non-classical light have been proposed. However, only a few experiments can be mentioned in the context of quantum memory [3], and efficient, reversible transfer of quantum information between different species has not yet been accomplished. An original protocol for a quantum, as well as classical, memory in solid state material is based on controlled reversible inhomogeneous broadening (CRIB) of a single atomic absorption line [4]. It requires an atomic ensemble with a large optical depth and a long optical coherence time. It also relies on the possibilities to prepare, through optical pumping, a narrow absorption line on a non-absorbing background, to broaden this line in a controlled and reversible way, and to apply a position dependent phase shift.

Erbium doped crystalline waveguides are interesting candidates for the realization of CRIB, as interaction lengths of many centimeters can be achieved, allowing for large absorption even at low doping concenration. In addition, the 1.53 μm, $^4I_{15/2} \rightarrow {}^4I_{13/2}$ transition in Erbium can feature coherence times in the ms range [5], and is well matched to standard telecommunication fibre, which allows future interfacing of such a memory with the standard telecommunication fibre network.

In this paper we report on the storage, recall and measurement of classical optical pulses via stimulated photon echoes [6], which provides an important test-bed for future quantum state storage based on CRIB. Furthermore, we present investigations of the linear dc-Stark effect for controlled broadening [7]. The experiments took advantage of Er^{3+} doped LiNbO$_3$ crystals with waveguiding structures, cooled to a temperature of around 3.5 Kelvin. While LiNbO$_3$ waveguides are extensively used in integrated optics, these are, to the best of our knowledge, the first studies in the context of all optical data storage.

Photon-echo based storage of classical light pulses

A common approach to storage and retrieval of light is based on three-pulse photon echo (3PE), also known as stimulated photon echo [6]. In this process a first, strong, optical *write* pulse excites the medium, creating an atomic coherence. The *data* pulses, a sequence of pulses encoding the information to be stored, are sent into the medium some time after the write pulse, which transfer the coherence into a frequency-dependent population grating in the ground and excited states. In order to retrieve the information, a third, strong, *read* pulse is used, which scatters off the grating and causes a photon echo to be emitted a time after the read pulse, which is equal to the time separation between write and data pulse [8]. If certain conditions for excitation energy and absorption depths are met, the echo is, to a high degree, an amplitude and phase replica of the stored data pulses.

Now, consider a data field consisting of two pulses (D1 and D2) with an amplitude ratio R and relative phase φ (see Fig. 1). The 3PEs appear at times $t_e = t_r + t_{Di} - t_w$ (i = 1, 2), where t_r is the arrival time of the readout, t_{Di} the arrival time of data pulse Di (i = 1, 2), and t_w the arrival time of the write pulse. The echoes will thus be dt = $t_{D2} - t_{D1}$ apart.

Because the efficiency of the 3PE is at best a few percent [9], much of the frequency-dependent popu-
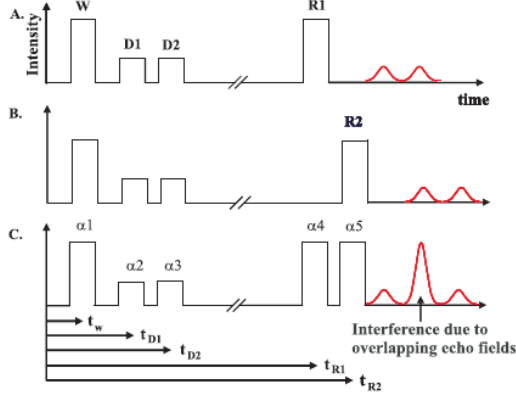
Fig. 1: Illustration of the sequence of pulses for the interference of photon echoes. The data is read out twice and the phase between the data (or read) pulses is changed to produce interference in the central time bin.

lation grating is preserved in the atomic ensemble after the read pulse. Therefore more echoes can be produced by sending in several read pulses. In our experiment, two subsequent read pulses were used to produce two copies of the data pulse. If we chose the distance between the read pulses to be dt, the same as the distance between the two data pulses D1 and D2, the echo of the second data pulse read out by the first read pulse (D2|R1), and the echo of the first data pulse read out by the second read pulse (D1|R2), will overlap and interfere (Fig. 1 c). The intensity of the echo in the central time interval (time-bin) is thus controlled by the phases of the write, the data and the read pulses, i.e. $\alpha1$, $\alpha2/3$, and $\alpha4/5$, respectively. This is true provided that the phase coherence or amplitude ratio is not perturbed partially or totally during storage and retrieval.

The sequence of two data pulses above is related to what is known in quantum communication as a time-bin qubit [10]. A time-bin qubit is a coherent superposition of a photon being in two time-bins, separated by a time difference long compared to the coherence time of the photon. It can be written as:

$$|\psi\rangle = c_0 |1,0\rangle + c_1 e^{i\varphi} |0,1\rangle, \qquad (1)$$

where $|1,0\rangle$ ($|0,1\rangle$) represents a photon in the first (the second, respectively) time-bin, and $\varphi = \alpha2 - \alpha3$ denotes their relative phase.

In the present experiment, classical (strong) coherent pulses were used, with width smaller than the temporal spacing dt between the two pulses; the state of light is thus described by a Poisson distribution of photons ($n \sim 10^8$), each of which is in the state described by Eq.1. Note that one could also describe our experiment as a setup containing two interferometers, as used for phase-coding quantum cryptography [1]: one interferometer prepares the time-bin qubits, i.e. here our two data pulses, while the second allows the projection measurement, i.e. our two read pulses.

Let us now describe the experimental setup. The output from an external-cavity cw diode laser was gated by a combined phase and intensity modulator, followed by an intensity modulator (both fibre optic). The first modulator was used to create the five excitation pulses and to apply phase shifts to some of the pulses, depending on the particular experiment. The second modulator was synchronized to the first one and used to improve the peak-to-background intensity ratio. The pulses were then amplified by an Erbium Doped Fiber Amplifier (EDFA). In order to obtain a good background suppression (>70 dB), the EDFA was followed by an acousto-optical modulator, which opened only for the series of pulses and suppressed light for all other times. The resulting pulses had durations of $t_{pulse}=15$ ns, with peak powers of around 5 mW for the write pulses, and around 1 mW for the other pulses. The first data pulse was created at $t_{D1} = 0.6\mu s$, the time between the data pulses was typically dt = 60ns and the read-out pulses were delayed with respect to the data pulses by 1 to 2 μs. The light was then coupled into an Er^{3+}-doped $LiNbO_3$ crystal (with waveguide, see below), which was cooled to 3.4 K by means of a pulse tube cooler. A magnetic field of about 0.2 Tesla was applied parallel to the C_3 axis. This reduces decoherence due to spectral diffusion [11], resulting in a coherence time T_2 of about 6 μs. Finally, the photon echoes were detected by a fast photo detector and displayed on an oscilloscope. The clock frequency was of 30 Hz, which ensured that all atomic excitations (featurig radiative a lifetime of 10 ms) had decayed between two subsequent storage/recall sequences.

The z-cut $LiNbO_3$ crystal was Erbium doped over a length of 10 mm by indiffusion of an evaporated 8 μm thick Er-layer at 1130°C for 150 h, leading to a Gaussian concentration profile of 8,2 μm 1/e penetration depth and $3.6 \times 10^{19} cm^{-3}$ surface concentration. The guiding channel was fabricated by indiffusion of a 7 μm wide, 98 nm thick Titanium-stripe at 1060°C for 8.5 h, resulting in a mono-mode guide with a mode size of 4.5x 3 μm FWHM intensity distribution [12]. The light was injected and collected with stan-
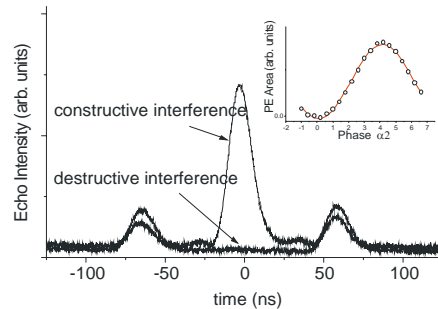
Fig. 2: Photon echo signals showing constructive and destructive interference. Inset: Central echo area as a function of phase.

dard optical fibers, which were butt coupled to the input and output of the waveguide.

In a first experiment, we varied the phase difference between the two data pulses. Figure 2 shows observed photon echoes in the case of constructive and destructive interference in the central time-bin, and the inset depicts the background subtracted area under the peak in the central bin as a function of the phase difference. Note that the background was of purely electronic origin and that no coherent or incoherent back- ground light was interfering with the echoes.

Figure 3 shows similar sinusoidal fringes, however, this time obtained through a phase change of the second read pulse. While this phase is scanned, the phase $\alpha 3$ of the second data pulse is kept constant at: 0, $\pi/2$, π, and $3\pi/2$, and all other phases are kept at zero. We observed an average visibility of 100% (within the experimental error). This experiment is conceptually analogous to preparing four different time-bin qubit states, which form two maximally conjugate bases, as is widely used in quantum cryptography in the so-called BB84 or four state protocol [13]. However, while in quantum cryptography set-ups the projection measurement is done with a widely unbalanced interferometer [1], we project the state with photon echoes using two read pulses. The photon echo process thus serves two purposes: storage/retrieval, and analysis of the state.

To further test the analogy between our photon-echo based interference scheme and a purely optical scheme, we measured the visibility V=(Max-Min)/(Max+Min) of the interference fringes for various ratios R of data pulse intensities. Note that the read pulses remained unchanged at equal intensity. In case of a purely optical measurement, the visibility of the interference should depend on R through

$$V = 2 \sqrt{R} /(1 + R). \qquad (2)$$

As depicted in Figure 4, the visibility in the photon-echo based read out reproduces indeed, within ex-
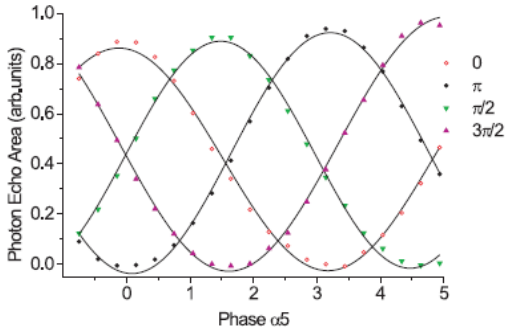
Fig. 3: Area under the central echo as function of the phase of the second read pulse. All four classical states, analogous to the quantum states used in the four-state quantum cryptography protocol, are stored, retrieved and analyzed with close to 100% fidelity.
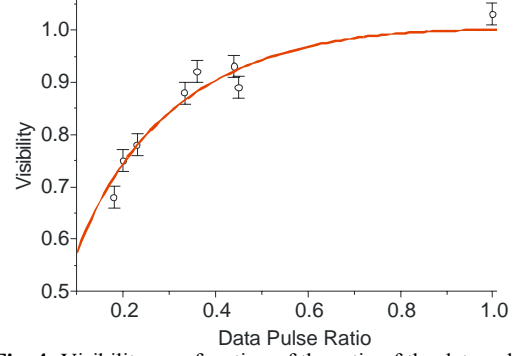
Fig. 4: Visibility as a function of the ratio of the data pulse intensities. Experimental points are in good agreement with the theoretical prediction, which contains no free parameter.

perimental error, the predictions for the optical setup.

We thus find that stimulated photon echoes do not only allow all-optical storage and readout, but also projection onto various bases, thereby replacing standard interferometric setups. The outstanding visibilities obtained in our measurements paired with the ease to extend our scheme to more than two read pulses (equivalent to more than two arms in an interferometer), or read pulses with different intensities (i.e. beam-splitters with variable splitting ratios) makes it a very interesting approach to storage (and readout) of quantum information. While our experiments have been performed with classical pulses and (low efficienct) traditional photon echoes, we believe that our scheme can be extended to highly efficient quantum state storage based on CRIB.

Controlled broadening based on Stark shifts
While photon-echo technology allows demonstrating and testing of key features required for quantum state storage, its limited efficiency of a few percent impacts on the use in quantum repeaters (however, see [14] for an approach based on multi-mode memories, which is promising for quantum memories with limited efficiency). A more efficient approach takes advantage of controlled reversible inhomogeneous broadening (CRIB) of a single absorption line [4].
A promising way to create controlled reversible broadening is based on the use of electric fields. In the presence of an external dc electric field, the energy levels of an atom with a permanent dipole moment are shifted; the linear dc-Stark effect. If the dipole moments are different for different electronic levels, this shift leads to a displacement of the associated optical transition frequency ω:

$$\Delta\omega\hbar =\Delta\mu_e\chi E \cos\theta \qquad (3)$$

Here $\Delta\mu_e$ is the difference between the permanent electric dipole moments of the two states connected by the transition, E is the applied dc electric field,

$\chi=(\varepsilon+2)/3$ is the Lorentz correction factor, ε is the dielectric constant of the sample, and θ is the angle between the vectors $\Delta\mu_e$ and E.

The linear dc-Stark effect can and has been observed in RE doped crystals through shifts of spectral holes [7,15], where the dipole moment in the ion is induced by local electric fields. However, no measurements have been reported on RE doped waveguides, neither crystalline nor amorphous.

In a crystal, because of the ordered structure of the crystalline lattice, the dipole moments are aligned along a set of one or more well defined directions. The symmetry of the crystal along with the site symmetry at the rare-earth-ion position determines the number of directions. All ions with vector $\Delta\mu_e$ aligned along the same direction experience the same shift in their resonance frequency with an applied electric field and thus the application of a DC electric field leads to a shift or splitting of the spectral hole, depending on the number of possible directions. The projection of $\Delta\mu_e$ between the two states, along the direction of the applied electric field, can be determined by measuring the shift of a spectral hole as a function of the electric field, as given by equation 3.

In our investigation we used a monochromatic laser to excite Er^{3+} ions from the lowest crystal field level of the $^4I_{15/2}$ ground state to the lowest crystal field level of the $^4I_{13/2}$ excited state, thereby creating a spectral hole at the frequency of the laser. We then decreased the laser intensity and scanned the frequency around the initial burning frequency three times while measuring the transmitted light as a function of time. Together with an independent time-to-frequency calibration of the laser scan, this yields three spectral hole profiles. During the first scan there was no applied electric field, for the second scan we applied an electric field across the sample, and for the third scan, we switched off the electric field to demonstrate the reversibility of the Stark induced line shift. See figure 5 for a graphical repre-

Fig. 5: Measurment sequence to assess magnitude and reversibility of the dc Stark shift.
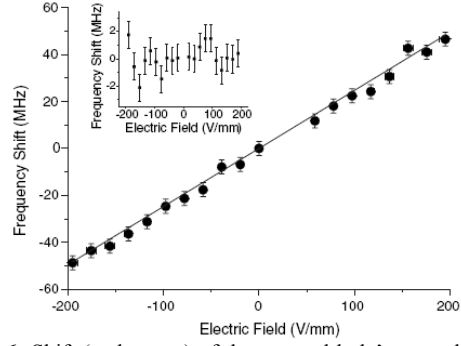
Fig. 6: Shift (and return) of the spectral hole's central frequency as a function of the electric field in the Erbium doped $LiNbO_3$ waveguide.

sentation of the measurement sequence.

The sample used in this investigation was a single domain, z-cut, $LiNbO_3$ crystal,1 mm thick, 6 mm long, and 6 mm wide, doped with Er^{3+} (0.5 at %), and MgO (5 mol %) and featuring single mode waveguides fabricated via proton-exchange. The sample was mounted between two metal electrodes spaced by 1 mm and cooled to 3.8 K. Light, linearly polarized along the crystal C_3 symmetry axis, was injected and collected with standard optical fibers. The C_3 symmetry axis was oriented parallel to the applied electric field and perpendicular to the light propagation direction. The inhomogeneous broadening in the sample is of around 250 GHz. We applied a magnetic field of approximately 0.7 T, parallel to the C_3 symmetry axis, to reduce the width of the spectral hole [11] by a factor of 5, yielding a hole width of 47 MHz, FWHM, which was largely dominated by power broadening. Note that the position of the spectral hole, which is the relevant parameter in our investigation, could be determined within a precision of ±3 MHz. We performed hole burning experiments as described above, with applied voltages ranging from -200 to 200 V, using a scannable cw external cavity diode laser at a wavelength of 1531.00 nm. To measure the spectral hole we scanned the laser over 1.2 GHz in 500 μs and measured the transmitted light with a photo detector.

The frequency shift of the spectral hole, relative to the zero field position, as a function of electric field is plotted in Fig. 6. The line is a linear fit to the data which passes through the point (0, 0). The dipole moment difference can be calculated from the slope of the line according to Eq. (3). We find an effective dipole moment difference $(\Delta\mu_e \, \chi)/(h) = 25 \pm 1$ kHz/(V cm^{-1}). The inset in Fig. 6 shows the position of the spectral hole measured after switching off the electric field for each applied field; the spectral hole returns to the initial zero field position. This, plus the opposite directional shifts that were observed with positive and negative voltages, confirms the reversibility of the Stark effect.

Conclusions

Our findings show that the relative phase and amplitude ratio of data pulses can be preserved during storage in the optical memory, and that storage can be combined with projection measurments, as required in quantum communication and computation schemes. While this result is based on experiments with classical pulses containing many photons, we expect that it can be extended to a more efficient approach to storage based on CRIB. Furthermore, we demonstrated the possibility to use the dc-Stark effect for controlled inhomogeneous broadening, which is key to quantum state storage based on CRIB. While more work is required, in particular concerning the preparation of a single, isolated absorption line on a non-absorbing background, our findings demonstrate the potential of $Er:LiNbO_3$ waveguides for quantum state storage compatible with the requirements of a telecommunication (quantum) network.

References

1 N. Gisin, G. Ribordy, W. Tittel, and H. Zbinden, Rev. Mod. Phys. **74**, 145 (2002).

2 H.J. Briege, W. Dürr, J.I. Cirac, and P. Zoller, Phys. Rev. Lett. **81**, 5932 (1998) .

3 B. Juulsgard *et al*., Nature **432**, 482 (2004), T. Chanelière *et al*., Nature **438**, 833 (2005), M.D. Eisaman *et al*., Nature **438**, 837 (2005).

4 M. Nilsson and S. Kröll, Optics Communications **247**, 393 (2005), B. Kraus *et al*, Phys. Rev. A **73**, 020302(R), A. Alexander *et al*, Phys. Rev. Lett. **96**, 043602 (2006), N. Sanguard *et al*., quant-ph/0611165.

5 T. Böttger, C.W. Thiel, Y. Sun, and R.L. Cone, Phys. Rev. B **73**, 075101 (2006).

6 T.W. Mossberg, Opt. Lett. 7, **77** (1982), M. Mitsunaga, Opt.and Quant. Electr. **25**, 1137 (1992), M. Staudt *et al*., quant-ph/0609201 (to be published in Phys. Rev. Lett).

7 S. Hastings-Simon *et al*, Opt. Comm. **266**, 716 (2006).

8 This simplified picture of a population grating is sufficient to describe our experiment, although remaining atomic coherences were a source of additional 2-pulse echoes. However, these echoes appear at different times compared to the 3PE and could be discarded via time-resolved detection.

9 T. Wang, C. Greiner, J. R. Bochinski, and T. W. Mossberg, Phys. Rev. A **60**, 757 (R) (1999).

10 J. Brendel, N. Gisin, W. Tittel, and H. Zbinden, Phys. Rev. Lett. **82**, 2594 (1999), W. Tittel and G. Weihs, Quant. Inf. Comp. **1**, 3 (2001).

11 Y. Sun et al, J. Lumin. **98**, 281 (2002).

12 I. Baumann *et al*., Appl. Phys. A **164**, 33 (1997) .

13 C.H. Bennett and G. Brassard, in Proceedings of the IEEE International Conference on Computers, Systems and Signal Processing, Bangalore, India (IEEE, New York, 1984), p. 175.

14 C. Simon et al, quant-ph/ 0701239.

15 K. Polgar, A.P. Skvortsov, Opt. Spectrosc. (USA) **58**, 140 (1985), A. Skvortsov, K. Polgar, L. Jastrabik, Radiat. Eff. Defect. Solid. **150**, 287 (1999).